Received: 23 January 2024 | Revised: 26 February 2024 | Accepted: 7 March 2024 | Published online: 11 March 2024

RESEARCH ARTICLE

Journal of Computational and Cognitive Engineering
2025, Vol. 4(3) 366–376
DOI: 10.47852/bonviewJCCE42022507

BON VIEW PUBLISHING

# Minimizing Urban Flooding by Optimal Design of Drainage System Using Sequential Least Squares Quadratic Programming and Spatial Datasets

**James O. Ekeh**[1] **and Manoj K. Jha**[2,*]

[1]*MKJHA Consulting, USA*

[2]*Department of Information Technology, University of Maryland Global Campus, USA*

**Abstract:** Urban flooding is caused due to poor drainage design and excessive rain. It severely affects the road infrastructure. Existing hydrologic software tools to examine the extent of urban flooding primarily require walking through a series of manual steps and address each study area individually, preventing a collective review of poor storm-drains in an efficient manner. Previous methods for optimal drainage design were inefficient and lacked the ability of solving the underlying optimization problem due to the inherent nonlinearity of the decision variables. In this paper, we develop a nonlinear optimization formulation to minimize urban flooding using underground pipe size as a decision variable. We propose a solution algorithm using sequential least squares quadratic programming and spatial datasets. The proposed method eliminates the need to examine each study area manually using existing hydrologic tools. An example using the storm-drain system for the Baltimore County is performed. The results show that the model is effective in identifying storm-drain deficiencies and correcting them by choosing appropriate storm-drain inlet types to minimize flooding. Future works may include using large datasets and a more sophisticated modeling approach for estimating rainfall intensity based on extreme weather patterns. The method can be applied to other jurisdictions if relevant hydrological and underdrain piping network data were available.

**Keywords:** urban flooding, stormwater runoff, storm-drain system deficiency, nonlinear optimization, sequential least squares quadratic programming (SLSQP)

## 1. Introduction

Urban flooding is a significant issue worldwide, which is primarily caused due to, among other things, storm-drain system deficiency associated with urban stormwater management and unusual weather patterns, such as excessive rain caused due to extreme events. Such disasters have surged in recent years. According to the Center for Research on the Epidemiology of Disasters and United Nations Office for Disaster Risk Reduction [1], over the last 20 years, 7,348 disaster events were recorded. These disasters claimed more than a million lives and led to about US$ 3 trillion in economic losses worldwide.

Many cities in the world have poor storm-drain design, which causes flooding due to excessive rain [2]. The situation exacerbates in the event of hurricanes or when the rain is more persistent and intense. The problem appears to be due to the lack of the drainage capacity of detention tanks and deficiency associated with pipe culvers in the event of rapid rain events.

With respect to storm-drain system deficiency, several methods have been proposed in the literature, including numerical simulation with a geographic information system [3], nature-based solution [4], bioretention [5], and smart stormwater management [6]. However, these methods either offer a qualitative discussion of the underlying issues or are hard to be adopted for real-world application. For example, Webber et al. [6] acknowledge that while data analytics and online optimization have been a topic of broad and well-developed research, often synthesized under the banner of hydroinformatics, limitation to current approaches remains. Developing optimization to the network scale and from the real-time perspective requires coordinated decentralized infrastructure. Guo [7] recommended a risk-based approach to the selection of design storm events, based on public perception, federal regulations, watershed physical characteristics, economics, and safety. The author discussed, at length, storm sewer system design and detention basin design. However, no optimization method was proposed to address storm-water system deficiencies.

There are a number of hydrologic modeling software (e.g., TR-55, HydroCAD, TR-20, HEC-RAS, StreamStats, L-THIA, SWMM, WMOST, MAST, HY-8) which are traditionally used to examine flood risks and make recommendations to address them. The first author undertook a number of flooding analysis using these software tools and reported the results in his dissertation [8]. Most of the available literature [3, 9–17] and the hydrologic software tools offer

*Corresponding author: Manoj K. Jha, Department of Information Technology, University of Maryland Global Campus, USA. Email: manoj.jha@faculty.umgc.edu

solutions to urban flooding either in a qualitative way or by iterating through a series of manual steps. This makes the process of identifying attributes causing flooding very inefficient. Furthermore, currently available literature on urban drainage design approaches the problem from a purely mathematical perspective, ignoring the geo-spatial analysis requirement to efficiently identify (preferably in real-time) and correct the drainage deficiency. For example, there are thousands of storm-drain pipes buried underground and it is not possible to analyze each of them individually unless there is an efficient procedure to analyze their combined effect collectively in understanding the likelihood of future flooding. In other words, while existing studies and hydrologic software tools are useful, they are primarily manual in nature requiring repetitive iterations to examine the effect of flooding due to certain rainfall intensity and watershed, cross-section, and culvert and piping characteristics.

Under this backdrop, the key contributions to this paper can be summarized as follows:

1) Develop a geo-spatial nonlinear optimization model by extracting spatial datasets on underground storm-drain pipelines to minimize flooding in a particular jurisdiction, such as a county, city, or municipality;
2) Perform the optimization by developing an integrated GIS-Python framework. The novelty of the GIS-Python integrated framework is that while the nonlinear aspect of the mathematical optimization can be performed in the Python environment, the optimal solution can be geocoded and passed to the GIS through a geo-spatial analysis. Such an approach advances the state of the art in curbing urban flooding, which has not been proposed in previous works. The other benefit is that the integrated GIS-Python framework enables us to work directly with the spatial datasets consisting of the piping network containing relevant information, such as pipe diameter, flow, slope, and roughness;
3) Bring the spatial datasets in the Python environment to perform the optimization. Upon optimization, deficient storm-drain pipes needing replacement can be quickly identified on a geographic map. The integrated GIS-Python framework is similar to the second author's work on GIS and genetic algorithms integration for highway route optimization [18] in that continuous bi-directional data transfer needs to take place to efficiently perform the optimization.

We have primarily focused on developing an optimization approach to solve a nonlinear optimization problem specific to storm-drain system deficiency. Pipe installation cost and other practical limitations in redesigning and installing storm-drain systems (e.g., budget constraints of a particular jurisdiction) have been skipped for future work. In recommending a new pipe size, we have followed guidelines by the Baltimore County, Maryland, USA.

## 2. Literature Review

Several studies have developed methods for assessing urban flooding and providing potential solutions. For example, Chang and Huang [19] proposed an emergy approach to assess urban flooding vulnerability. Cherqui et al. [20] developed risk reduction measures due to flooding. Kim et al. [21] developed a decision-making tool for urban flooding under climate change. Xie et al. [22] performed an integrated assessment of urban flooding mitigation strategies. Zhou et al. [23] established a linkage between urban extreme rainfall and urban flooding in China. The US Environmental Protection Agency (EPA) has developed a national stormwater calculator to estimate the annual amount of rainwater and frequency of runoff from a specific site [24]. ScienceDirect has compiled a list of papers under the title "Urban Flooding" [3, 9–17]. These papers discuss a range of issues related to urban flooding, including urban flood management and relationships to climate change and urban flooding.

Flynn and Davidson [25] discussed the issues associated with poor storm-drain design. They concluded that despite major investments in stormwater infrastructure, urban areas continue to experience urban flooding. Municipal stormwater management plans in many developed countries have favored the use of gray infrastructure (e.g., sewer separation projects, deep storage tunnels, and regional treatment facilities). These engineering solutions can be costly, tend to promote centralized subsurface conveyance systems with end-of-pipe treatment, and often take years to complete. Despite major investments in stormwater infrastructure, urban areas continue to experience critical problems in managing water flows, including flooding, surface water impairment, and combined sewer overflows. While the study outlined the causes of urban flooding (e.g., stormwater system deficiencies) well, it did not offer any solution, much less, a real-time optimization solution to address stormwater system deficiencies.

Many studies have proposed green infrastructure and bioretention to curb urban flooding [5, 26–28]. However, there may be practical limitations for actual implementation of green infrastructure and bioretention, including limited resources available to counties, cities, and municipalities.

Some studies have been reported on numerical methods for drainage culvert redesign. For example, Duan et al. [29] developed a multiobjective approach for the design of detention tanks in the urban stormwater drainage system. Jun et al. [30] developed a storm-drain-based bivariate frequency analysis method to design urban storm-drains. Selbig et al. [31] investigated the effect of particle size distribution on the design of urban stormwater control measures. Monrabal-Martinez et al. [32] investigated the seasonal variation in pollutant concentrations and particle size distribution in urban stormwater design. Chen et al. [33] developed a tool for urban rainwater management using integrated design workflow. However, these methods could not work directly with spatial datasets limiting their practical applicability in performing a tradeoff analysis or optimization in identifying deficient underground piping structure.

### 2.1. Current state of the art in urban drainage design

Some relevant previous works on optimal drainage design can be found in Mays [34], Taur et al. [35], and Afshar [36]. Mays [34] developed a mathematical optimization method for determining the optimal layout and design of storm sewer systems. However, the method required manual datasets as inputs preventing efficient real-world applicability of the developed methodology. Moreover, the programming languages used to solve the mathematical problem were old and outdated, which further limited the practical applicability of the developed methodology. Newer and more sophisticated programming techniques have emerged since 1971, which can work directly with spatial datasets enhancing the practical applicability and real-time implementation.

The methods proposed in other studies had the inability of handling either the nonlinearity associated with the decision variables or working with spatial datasets of underground storm-drains in performing offline or online optimization to identify and correct culvert piping deficiencies. The studies primarily focused on solution procedures. They proposed numerical methods and iterative heuristics, such as dynamic programming and particle swarm optimization. Moreover, the studies approached the problem of piping optimality from a pure mathematical perspective and ignored the geo-spatial analysis needed for an efficient practical implementation, preferably in real-time, as suggested by Webber et al. [6].

The majority of the literature on optimal drainage system design is qualitative in nature. While some of them [3, 29] discuss analytical and mathematical approaches for urban flood management, the approaches are still manual since one must go through a series of manual steps to examine each storm-drain outlet individually. This process is very time consuming and cannot ensure a reduction in flooding in each urban segment since the direction of flow of water cannot be collectively examined.

## 3. Methodology

The hydrologic technique most often used in urban drainage design is the rational method expressed as [7]:

$$Q = CIA \tag{1}$$

Where:

$Q$ = peak discharge ($m^3/s$)
$C$ = runoff coefficient
$I$ = design storm rainfall intensity (mm/hr)
$A$ = drainage area (hectares)

The quantity, $I$, can be further formulated as a function of extreme weather as follows:

$$I = I(ew) \tag{2}$$

Using the TR-55 method, peak discharge, runoff depth, initial abstraction, unit peak discharge, and pond/swamp factor can be computed as follows:

$$Q_P = Q_u A Q F_p \tag{3}$$

$$Q = \frac{(P - I_a)^2}{P - I_a + s} \tag{4}$$

$$I_a = 0.2s \tag{5}$$

$$s = \frac{1000}{CN} - 10 \tag{6}$$

$$Q_u = f\left(T_C, \frac{I_a}{P}, \text{ Rainfall Distribution Type}\right) \tag{7}$$

$$F_p = f(\%\ \text{Ponds and Swamps}) \tag{8}$$

where $A$ = total watershed area ($mile^2$); $C_N$ = overall curve number for the watershed; $Fp$ = pond and swamp adjustment factor; $I_a$ = initial abstraction (inch) losses before runoff begins (surface depressions, interception by leaves, evaporation, infiltration); $P$ = precipitation (inch) for 24-hr duration storm of return period for which the study is interested; $Q$ = depth of runoff over entire watershed (inch); $Q_p$ = peak discharge (cfs); $Q_u$ = unit peak discharge (cfs/$mile^2$-inch); $s$ = potential maximum watershed water retention after runoff begins (inch); $T_c$ = time of concentration for the watershed (hr); time for runoff to travel from the furthest distance (by time) in the watershed to the location where to be determined $Q_p$.

$I_a$ can be further defined as a function of extreme weather as:

$$I_a = I_a(ew) \tag{9}$$

There are typically three distinct runoff patterns in a watershed: sheet flow, shallow concentrated flow, and channel flow. Each of the flow patterns requires a unique mathematical expression as follows:

$$T_c = T_{t(sheet)} + T_{t(shallow\ concentrated)} + T_{t(channel)} \tag{10}$$

$$\text{Sheet Flow}: \ T_t = \frac{0.007(nL)^{0.8}}{(P_2)^{0.5} S^{0.4}} \tag{11}$$

$$\text{Shallow Concentrated Flow}: \ T_t = \frac{L}{3600V} \tag{12}$$

$$\text{If paved surface}, \ V = 20.3282 S^{0.5}; \text{Unpaved}: V = 16.1345 S^{0.5} \tag{13}$$

$$\text{Channel Flow}: \ T_t = \frac{L}{3600\ V}; \quad V = \frac{1.49}{n} R^{2/3} S^{0.5} \ (\text{Manning Equation}) \tag{14}$$

where $L$ = length of flow pattern (ft) (includes all wiggles in channels); $n$ = *Manning's* $n$ value; for sheet flow, $n$ represents the ground cover to a depth of about 1.2 inches (3 cm); for channel flow, $n$ represents bank full conditions for an open channel or full conditions for a culvert; $P_2$ = 2-yr return period, 24-hr duration precipitation for the geographic region where your watershed is located (inch); $R$ = hydraulic radius (ft) of bank full open channel or culvert flowing full (computed automatically if channel cross-section dimensions are input); $S$ = average ground slope of each flow pattern (ft vertical/ft horizontal); $T_c$ = time of concentration for the watershed (hr); time for runoff to travel from the furthest distance (by time) in the watershed to the location where you wish to determine $Q_p$; $T_t$ = travel time for flow regime of interest (hr) – sheet, shallow concentrated, or channel flow; $V$ = average velocity of water in each flow regime (ft/s).

Based on the above formulation, it is obvious that amount of flooding will depend on discharge rate, rate of rainfall, land characteristics, and volume of the storm-drain to allow for proper drainage of rainwater. Therefore, conceptually, the flood minimization problem can be formulated as:

$$\text{Min } F = f(Q, T, L, S, V) \tag{15}$$

where $F$ = Flooding ($m^3$); $Q$ = discharge rate ($m^3$/sec); $T$ = length of time of rain (sec); $L$= land characteristics (e.g., impervious, grassy, other soil type, etc.); $V$ = volume of the storm-drain ($m^3$/sec); and $S$ = slope.

A hypothetical relationship for $F$ can be expressed as:

$$F = \alpha \frac{(Q - V)TL}{S} \tag{16}$$

where α is a constant.

The purpose of Equations (15)–(16) is to illustrate, conceptually, the independent variables which may influence the flooding. These equations, however by no means, represent an exact relationship between the dependent variable, $F$, and the independent variables. It can be observed from these equations that the higher the difference between discharge rate and storm-drain volume, the higher the flooding. Likewise, longer rain duration, smaller storm-drain volume, larger impervious areas, and smaller slopes will tend to increase the flooding. Models from the National Oceanographic and Atmospheric Administration (NOAA) can be used to estimate appropriate rainfall intensity.

Many books, articles, and manuals have been written on stormwater conveyance modeling and design. For example, Durrans et al. [37] and Guo [7] discuss design considerations with respect to storm-drain systems. However, as discussed previously, available methods for storm-drain system design do not offer an optimization procedure for an enhanced tradeoff analysis limiting the practical implementation of the methods. In this paper, our goal is to develop an optimization procedure to minimize flooding using storm-drain inlet design variables to perform a quick tradeoff analysis for an enhanced practical implementation.

Storm-drain system deficiency means inability of the storm-drain to be effective in stormwater runoff conveyance. This relates to poor design of the stormwater inlet systems and waterways, such as channels, conduits, swales, and drainage paths. The decision variables in the proposed optimization procedure may include rainfall intensity, land characteristics (e.g., gray v. green infrastructure, impervious, grassy, other soil type, etc.), and design variables for the storm-drain (including constrains placed on the design variables). For example, effective radius ($R$) of various sizes of box culverts can be considered as a design variable. In order to develop the optimization formulation, we re-label Equation (17) as:

$$Q_1 = CIA_w \tag{17}$$

The *Manning* equation to calculate the outflow to a particular storm-drain inlet is expressed as [7, 37]:

$$Q_2 = \frac{KA_sR^{2/3}S^{1/2}}{n} \tag{18}$$

where $A_s$ = area of the storm-drain; $R$ = hydraulic radius; $S$ = slope of the storm-drain inlet; $K$ = unit conversion factor (1.49 for English units and 1 for SI units); and $n$ = *Manning* coefficient.

From the inspection of Equations (17) and (18), it is clear that flooding will occur if: $Q_1 > Q_2$; and flooding will not occur if $Q_1 \leq Q_2$. Therefore, for minimizing flooding, following condition should be satisfied:

$$CIA_w \leq \frac{KA_sR^{2/3}S^{1/2}}{n} \tag{19}$$

In a special case of circular storm-drain pipe, the pipe area can be represented as $\frac{\pi D^2}{4}$ and the hydraulic radius as $\frac{D}{4}$ where $D$ is the pipe diameter in mm. Using these values, Equation (19) will reduce to

$$CIA_w \leq \frac{2K\pi D^{\frac{8}{3}}S^{\frac{1}{2}}}{12 \times n} = \frac{K\pi D^{\frac{8}{3}}S^{\frac{1}{2}}}{6n} \tag{20}$$

or

$$I \leq \frac{K\pi D^{8/3}S^{1/2}}{6CA_wn} \tag{21}$$

Assuming everything else to be a constant for a given watershed will lead to the following situation:

$$I \leq \frac{\beta D^{8/3}}{A_w} \tag{22}$$

where $\beta$ is a constant, $I$ = rainfall intensity; $D$ = inlet pipe size (or diameter); and $A_w$ = area of the watershed.

## 3.1. Rainfall intensity and conversion of rainfall to runoff

Many studies have been reported on future changes in extreme precipitation by employing climate models. For example, Tamm et al. [38] expressed the need for frequent update of intensity–duration–frequency curves for a more realistic calculation of rainfall intensity for designing urban drainage system. Such an update is a topic of research on its own and beyond the scope of this study, which is to develop a mathematical methodology to handle the nonlinearity associated with storm-drain conveyance system design. Once a more realistic rainfall intensity is available through advanced modeling techniques, it can be plugged into the proposed methodology developed here.

The maximum 24-hour rainfall intensity can be obtained from NOAA graphs. The runoff volume can be calculated using the curve number (CN) method [39]. The CN equation is a relationship between runoff volume and rain volume. The major factors that determine CN are the hydrologic soil group, cover type, treatment, hydrologic condition, and antecedent runoff condition. Another important factor is whether impervious areas outlet directly to the drainage system or the flow spreads over previous areas before entering the drainage system.

In the proposed research, we have made certain simplifying assumptions in calculating runoff volume from rainfall intensity and have used a deterministic interpretation of the rational method, which does not convert the rainfall frequency to the same runoff frequency. While this issue will affect the optimization and can be addressed in future works, we believe our method still captures the worst-case scenario in optimizing the pipe dimensions since any loss in runoff volume is neglected.

## 3.2. Nonlinear optimization with sequential least squares quadratic programming (SLSQP)

An inspection of Equation (22) reveals that because the rainfall intensity varies nonlinearly with the pipe diameter, it is a nonlinear optimization problem. While there are many methods available to solve nonlinear problems, sequential quadratic programming (SQP) has become the most successful method in solving nonlinearly constrained optimization problems [40]. SQP solves a sequence of optimization subproblems, each of which optimizes a quadratic model of the objective subject to a linear equivalent of the constraints. If the problem is unconstrained, then the method reduces to Newton's method for finding a point where the gradient of the objective vanishes. If the problem has only equality constraints, then the method is equivalent to applying Newton's method to the first-order optimality conditions, or Karush–Kuhn–Tucker conditions, of the problem. Further details on the mathematical foundations of SQP can be found in standard references and have been skipped here for brevity.

SLSQP is an extension of SQP method in which the original problem is replaced with a sequence of quadratic problems whose objectives are second-order approximations of the Lagrangian and whose constraints are the linearized original constraints. It uses certain globalization techniques to guarantee convergence irrespective of the initial point.

The SLSQP is encoded into the Python programming environment via the package called *scipy.optimize*. The *minimize* function provides a common interface to unconstrained and constrained minimization algorithms for multivariate scalar functions in *scipy.optimize*. To demonstrate the minimization function, the following nonlinear optimization problem is considered as an illustration:

$$Min\ Z = x_1 x_4 (x_1 + x_2 + x_3) + x_3 \tag{23}$$

subject to

$$x_1 x_2 x_3 x_4 \geq 25 \tag{24}$$

$$x_1 + x_2 + x_{23} + x_4 = 40 \tag{25}$$

$$1 \leq x_1, x_2, x_3, x_4 \leq 5 \tag{26}$$

$$x_0 = (1, 5, 5, 1) \tag{27}$$

where $Z$ is the objective function; and $x_1$, $x_2$, $x_3$, and $x_4$ are the decision variables for the conceptual optimization problem. This problem has a nonlinear objective that the optimizer attempts to minimize. The nonlinear nature of the objective function is obvious by the left-hand side of Equation (23) where degree of the decision variables is 4. The decision variable values at the optimal solution are subject to both equality (= 40) and inequality (≥ 25) constraints presented in Equations (24) and (25), respectively. The product of the four decision variables must be greater than 25 while the sum of squares of the variables must also equal 40. In addition, all variables must be between 1 and 5 and the initial guess is $x_1 = 1$, $x_2 = 5$, $x_3 = 5$, and $x_4 = 1$.

Using the above illustrative nonlinear optimization problem as a guide, an optimization procedure is developed in Python using SLSQP solver to solve the nonlinear optimization problem for our study. This solver, which is based on the principles of sequential least squares, is a package within Python's model called *Scipy.optimize*. In Figures 1–2, the Python code snippets show the application of this solver to the current nonlinear optimization problem.

**Figure 1**
**First Python code screenshot showing application of SLSQP**

```
[399]: # minimization problem Eqs. (4.28)-(4.30)
       # FIRST SCENERIO, i_r=0.277
       # SECOND SCENERIO, i_r=0.05
       #x[0]=pipe diameter in inches, this is the first decision variable
       #x[1]=Watershed area in sq. ft.
       c=0.84 # runoff coefficient, can be changed as desired
       i_r=0.277 # First Scenerio
       #i_r=0.05 # Second scenerio
       s_0=2 # slope
       n_r=0.012 # roughness, can be changed as desired
       def objective(x):
           a_2=((x[0]**2)*0.25*(22/7))/144 # This is the area of the pipe in ft.^2
           r_h=x[0]/48 # Hydraulic radius, in ft.
           q_2=(a_2*(r_h**(2/3))*(s_0**0.5))/n_r # this is Manning's Equation, flow rate is in cfs
           q_1=c*i_r*x[1] # This is the rational method, flow rate is in cfs
           return (q_1-q_2)

       def constraint1(x):
           return x[0]-2.0

       def constraint2(x):
           a_2=((x[0]**2)*0.25*(22/7))/144 # This is the area of the pipe in ft.^2
           r_h=x[0]/48 # Hydraulic radius, in ft.
           q_2=(a_2*(r_h**(2/3))*(s_0**0.5))/n_r # this is Manning's Equation, flow rate is in cfs
           q_1=c*i_r*x[1] # This is the rational method, flow rate is in cfs
           return (q_2-q_1)-0

[400]: # initial guesses
       n = 2 # this means there are two decision variables
       x0 = np.zeros(n)
       x0[0] = 2 # This is the initial value of the pipe diameter in inches
       x0[1]=10000 # This is the initial value of the watershed area in sq. ft.

[401]: # show initial objective
       print('Initial Flooding rate in cfs: ' + str(objective(x0)))

       Initial Flooding rate in cfs: 2326.490860092466
```

**Figure 2**
**Second Python code screenshot showing application of SLSQP**

```
[402]: # optimize
       b1 = (2,100) # this is the allowable range of pipe sizes which can be changed
       b2=(10000,100000) # this is the allowable range of watershed area in sq. ft. which can be changed.
       bnds = (b1,b2)
       con1 = {'type': 'ineq', 'fun': constraint1}
       con2 = {'type': 'eq', 'fun': constraint2}
       cons = ([con1,con2])
       solution = minimize(objective,x0,method='SLSQP',\
                           bounds=bnds,constraints=cons)

[403]: x = solution.x

[404]: # show final objective
       print('Minimum Flooding:  ' + str(objective(x)))

       Minimum Flooding: 1.3642420526593924e-12

[405]: # print solution
       print('Solution')
       print('Optimial Pipe Size = ' + str(x[0]))
       print('Optimal Watershed Area = ' + str(x[1]))

       Solution
       Optimial Pipe Size = 56.85340635515565
       Optimal Watershed Area = 10000.000083007115
```

## 4. Case Study Example

We apply the proposed methodology to an underground storm-drain piping network for Baltimore County, Maryland. A sample section of the network is shown in Figure 3.

The spatial dataset for this study is obtained from the website of the Environmental Systems Research Institute. It is available in ESRI's ArcGIS portal using the following code:

Storm_drain = gis.content.get('07d6eb057e554c51832c4f0852ecf9c0')

The map in Figure 3 has 131,817 storm-drain pipes with information on velocity, length, height, width, slope, flow rate, and some other relevant features. However, in many instances there are missing values, and the data are not complete. For example, in 50,309 instances velocity information is missing and in 20,817 instances pipe diameters are missing. The storm-drain pipe shapes are arched, circular, oval (elliptical), and rectangular. For a special case of circular pipes and after pruning missing, unknown, and unrealistic values, the dataset reduces to 64,719. We plot three sets of data to gain insight to the piping database: (1) velocity v. flow rate; (2) design length v. flow rate; and (3) geometric shape v. velocity. These plots are shown in Figures 4–6, respectively. The plot of velocity v. flow rate (Figure 4) shows that most of the pipes have a velocity between 0 and 15 mps (0–50 fps) and corresponding flow rate between 0 and 11 $m^3$ per sec (0–400 cfs). The plot of design length v. flow rate (Figure 5) shows that most of the pipes have a design length between 0 and 180 m (591 ft). The plot of geometric slope and velocity (Figure 6) shows that most of the pipes have a geometric slope between 0 and 25. While, in general, a higher slope would lead to a higher velocity, the plot may be skewed due to some outliers or inconsistent data. Any inconsistency is attributed to the inconsistency in the spatial dataset. There may be some outliers or inaccurate data that are not recorded correctly.

The optimization is performed in Python for a rainfall intensity of 7.04 mm per hour (0.277 inch per hour) obtained from NOAA charts for Baltimore. Because the optimization procedure is nonlinear, an initialization step is necessary. In the initialization step, certain dummy initial variables are used based on which initial flooding rate is calculated. Two examples are performed. The following input values are considered for the first example: runoff

**Figure 3**
**Sample storm-drain section for Baltimore County**


**Figure 5**
**Plot of design length v. flow rate for the Baltimore County storm-drain spatial dataset**

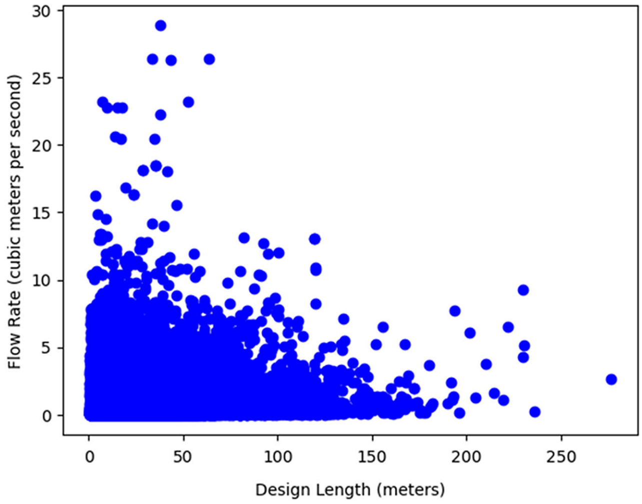


**Figure 4**
**Plot of velocity v. flow rate for the Baltimore County storm-drain spatial dataset**

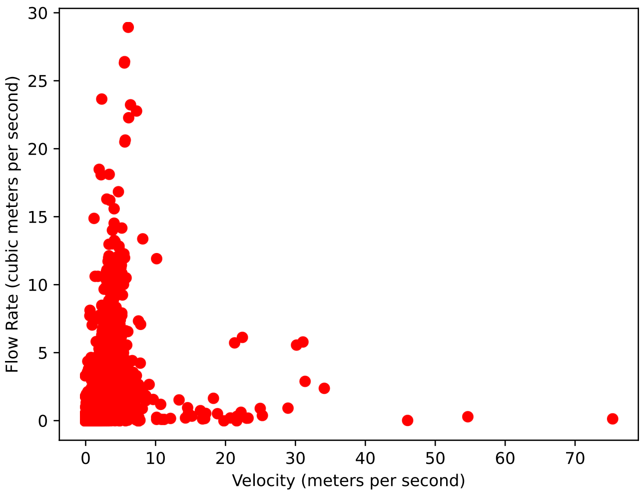


**Figure 6**
**Plot of geometric slope v. velocity for the Baltimore County storm-drain spatial dataset**

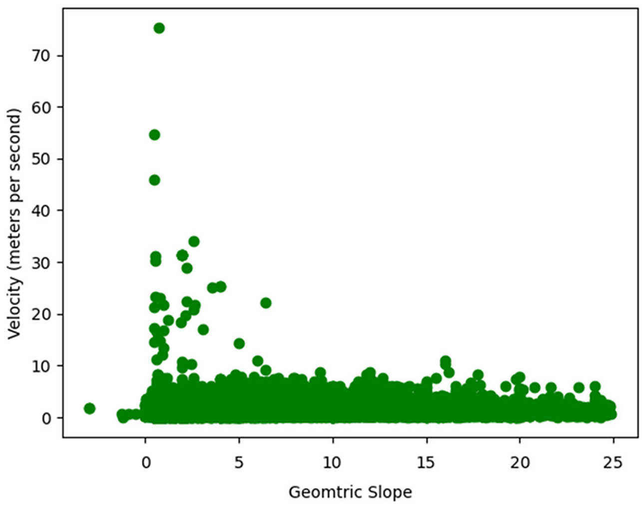


coefficient = 0.84; rainfall intensity = 7.04 mm per hour (0.277 inches per hour); geometric slope = 2%; roughness = 0.012; initial value of the pipe diameter = 50.8 mm (2 inches); initial value of the watershed area = 0.093 hectare (10,000 sq. ft.); allowable bounds of pipe size in mm = [50.8–2,540] (in inches=[2–100]); and allowable bounds of the watershed in $m^2$ = [929.03–9,290.3] (in sq. ft. = [10000–100000]).

Using the above values, initial flooding is obtained to be 65.89 $m^3$ per sec (2,326.49 cfs). After optimization with the SLSQP approach is performed, an optimal pipe size for a no flood situation is obtained to be 1,443.99 mm (56.85 inches). Another example with a rainfall intensity of 1.27 mm per hour (0.05 inches per hour) is performed, which results in an initial flooding of 11.88 $m^3$ per sec (419.69 cfs) and optimal pipe size of 760 mm (29.92 inches).

A comparison of both sets of results shows that an underestimated value of rainfall intensity may result in a reduced optimal pipe size. Therefore, it makes sense to use a realistic value of the rainfall intensity using most up-to-date NOAA data or more sophisticated climate models to obtain better results.

A plot of geometric slope v. initial flooding is shown in Figure 7. It can be seen that as the slope increases initial flooding decreases. It means that it may not be necessary to optimize the pipe size for locations with higher slopes since the risk of flooding is less. Next, a sensitivity analysis is performed to examine the variation among rainfall intensity, flooding, and optimal pipe size.

The result is shown in Table 1. It can be observed that in general, flooding increases as the rainfall intensity increases. This is a common natural phenomenon. Regardless of how adequately

**Figure 7**
**Plot of geometric slope v. initial flooding rate**

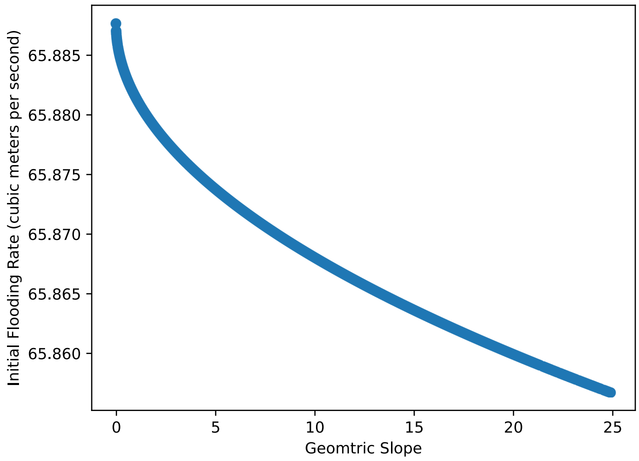


**Figure 8**
**Aerial view of Jones Falls watershed**

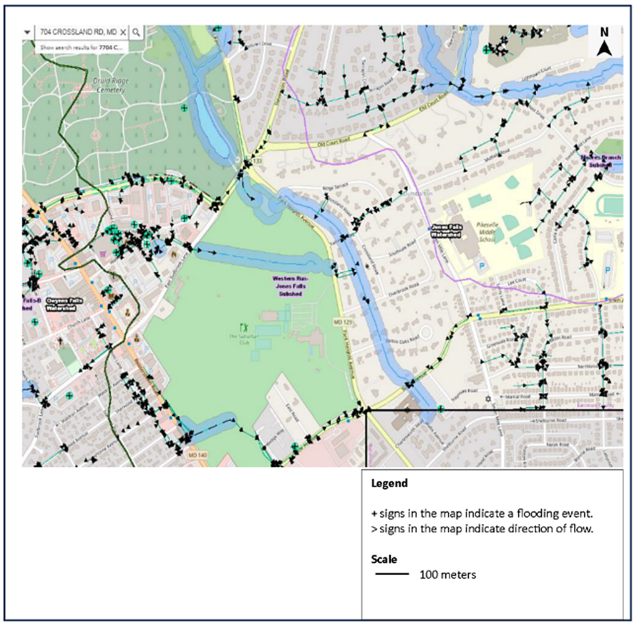


**Table 1**
**Variations among rainfall intensity, flooding, and optimal pipe size**

| Rainfall intensity (mm/hr) | Flooding in m$^3$ for a fixed pipe size of 1,270 mm | Optimal pipe size (mm) to minimize flooding |
|---|---|---|
| 6.35 | 12.69 | 1397 |
| 8.89 | 36.47 | 1600.2 |
| 11.43 | 60.26 | 1752.6 |
| 13.97 | 84.05 | 1879.6 |
| 16.51 | 107.83 | 2006.6 |
| 19.05 | 131.62 | 2108.2 |
| 21.59 | 155.41 | 2209.8 |
| 24.13 | 179.19 | 2311.4 |
| 26.67 | 202.98 | 2387.6 |

underground piping network is designed, extreme weather patterns and excessive rain events will tend to create flooding. While adjustments to rainfall intensity have been left for future works, our algorithm takes into account the worst-case scenario to optimize pipe size to minimize flowing as illustrated by the screenshots in Figures 1–2. In general, a large pipe size is required to minimize flooding.

Using the optimization algorithm, a revised pipe size (rounded off to the nearest integer) can be obtained for the 131,817 pipes. For incomplete and missing values in the dataset, appropriate data pruning, imputing, or cleansing should be performed before applying the optimization model for practical implementation.

As an illustrative real-world example, the flooding risk, amount of runoff, and existing underground pipe sizes along certain streets in the Jones Falls watershed in Baltimore County are performed. Figure 8 shows the aerial view of the watershed at 704 Crossland Road, Pikesville, MD. Figure 9 shows the number of flooding events and amount of runoff for Jones Falls watershed.

For the period of 2005–2015, collectively, the region experienced 230 flooding events with the highest number of flooding events experienced along Slade Avenue. Currently, Slade Avenue has a circular underground pipe of 609.6 mm (24 inches). Upon optimization, a new optimal pipe size is obtained for the underground pipes that would minimize flooding. The result is shown in Table 2. For Slade Avenue, a pipe size of 2,133.6 mm (84 in) is recommended. A similar analysis can be performed for a particular watershed or region and results can be cross-checked against the existing manual procedures, such as using TR-55.

## 5. Practical Implementation of the Developed Approach

Unlike the detailed mathematical calculations to be undertaken manually for storm-drain design (e.g., the methods proposed in Guo [7] and Durrans et al. [37]), the approach developed here is easy to implement. The Python code module automatically extracts the geo-spatial database containing information on underground storm-drain network and performs necessary optimization to recommend pipes to minimize flooding events. The model can easily be implemented to any jurisdiction if geo-spatial datasets were available in appropriate format. A dashboard for monitoring flooding events in real-time can be developed in future works. This will either help avoid catastrophic failures or take timely mitigation measures to reduce collateral damage due to sudden and unforeseen flooding events. One caveat for actual implementation would be budget and resource constraints of a particular jurisdiction since replacing deficient stormwater lines is costly.

### 5.1. Computational challenges with SLSQP

For the example studies performed in the current research, there were no computational challenges encountered while handling the nonlinear optimization problem with SLSQP and spatial datasets. This is because we were only dealing with numerical computation with less than a million-piping network. It is anticipated that when non-numerical spatial computations with over a million datasets are involved and if the computation must be performed in real-time, the computation process may slow down a little bit. We discussed this issue in the highway alignment context in one of our previous works [18]. For the present problem, this issue can be addressed in

**Figure 9**
**Number of flooding events and amount of runoff in Jones Falls watershed between 2005 and 2015**

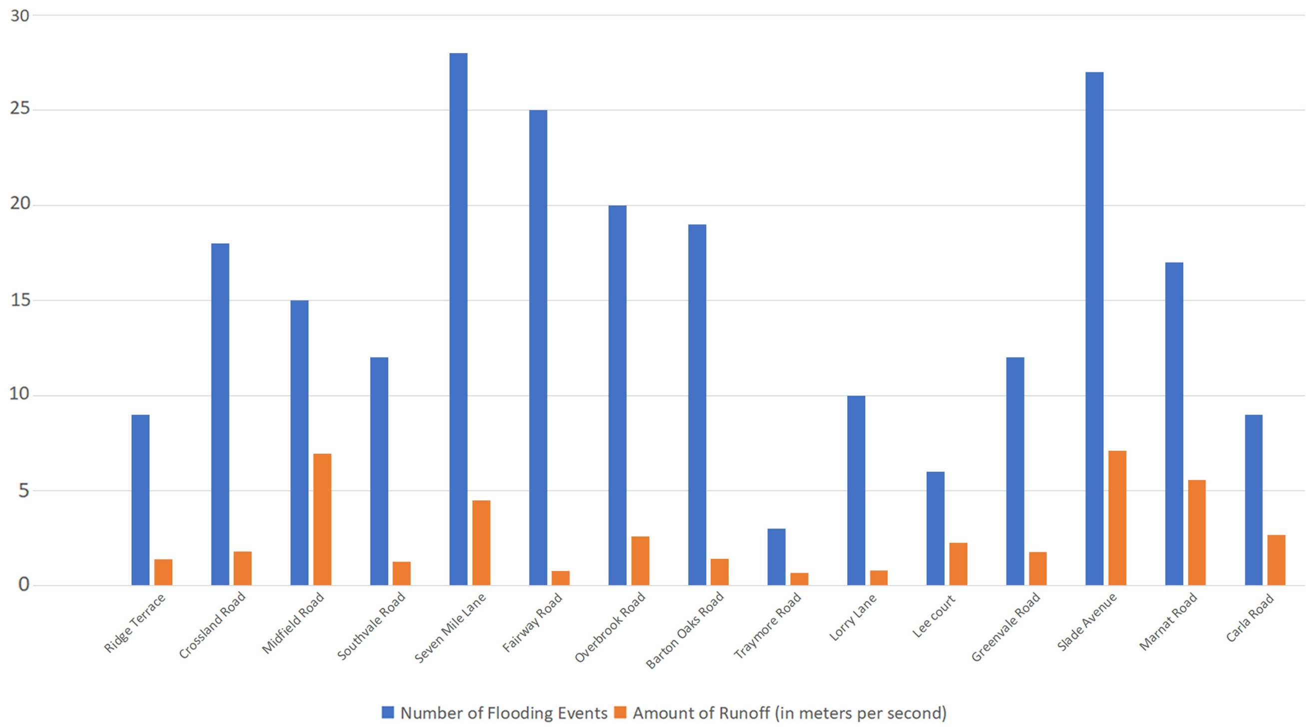


**Table 2**
**Optimal pipe size for Jones Falls watershed to minimize flooding**

| Pipe number | Street name | Number of flooding | **Discharge rate ($m^3$ per sec)** | Underground culvert diameter (if available) in mm | Adjusted (optimal) diameter in mm |
|---|---|---|---|---|---|
| 1 | Ridge Terrace | 9 | 1.39 | NA | 1118 |
| 2 | Crossland Road | 18 | 1.81 | 457 | 1372 |
| 3 | Midfield Road | 15 | 6.94 | Corrugated metal pipe (CMP) 1067 × 686 Elliptical | 1220 × 2134 |
| 4 | Southvale Road | 12 | 1.27 | NA | 914 |
| 5 | Seven Mile Lane | 28 | 4.47 | 914 | 1829 |
| 6 | Fairway Road | 25 | 0.76 | Reinforced round concrete pipe (RRCP) 1067 × 686 Elliptical | 1220 × 2134 |
| 7 | Overbrook Road | 20 | 2.61 | 381 Circular | 1829 |
| 8 | Barton Oaks Road | 19 | 1.42 | NA | 1067 |
| 9 | Traymore Road | 3 | 0.68 | NA | 533 |
| 10 | Lorry Lane | 10 | 0.79 | 533 Circular | 686 |
| 11 | Lee court | 6 | 2.27 | 457 Circular | 1676 |
| 12 | Greenvale Road | 12 | 1.78 | 381 Circular | 1372 |
| 13 | Slade Avenue | 27 | 7.11 | 610 Circular | 25 |
| 14 | Marnat Road | 17 | 5.55 | 914 Circular | 1829 |
| 15 | Carla Road | 9 | 2.66 | 457 Circular | 2134 |

future works when dealing with large spatial datasets and when performing the computation in real-time.

## 6. Conclusions and Future Works

This paper formulated a nonlinear mathematical optimization problem using SLSQP and spatial datasets to address the flooding on urban roadways due to deficient storm-drain pipe geometry. The study was carried out to investigate the optimal culvert capacity associated with the hydraulic analysis that could justify the sizing of the pipe culvert to minimize flooding. Based on the sample results, it is shown that the GIS and Python-based nonlinear optimization model within a Python environment is an effective tool in identifying storm-drain deficiencies and correcting them by choosing appropriate storm-drain inlet types to minimize flooding. Moreover, the developed procedure eliminates the need to perform manual analysis using existing hydrologic software tools, although those tools can still be used in subsequent stages for micro-level manual analysis.

The results show that deficient and poor design of storm-drain pipes are key contributors to urban flooding. For the Baltimore County case study, flooding was attributed to the difference between in-flow and out-flow. Whenever there was excess in-flow, a flooding scenario was observed. This scenario was removed by performing the nonlinear optimization and selecting optimal pipe sizes.

While the proposed approach identifies corrections to the storm-drain pipeline network, challenges with respect to cost and other resources to replace the poor piping network are not explored in this study. Future works may include expanding the nonlinear optimization methodology on larger datasets with complex hydrological features as well as modeling the spatial disparity when considering the effects of extreme weather and climate change. Additional sensitivity analysis for a range of input values, such as roughness, geometric slope, and watershed area, can also be undertaken in future works. The future works may also include expanding the formulation to include the nonlinearity associated with the conversion of rainfall intensity to runoff volume as well as performing the optimization in real-time. The method can be applied to other jurisdictions if relevant hydrological and underdrain piping network data were available.

## Conflicts of Interest

Manoj K. Jha is an Associate Editor for *Journal of Computational and Cognitive Engineering*, and was not involved in the editorial review or the decision to publish this article. The authors declare that they have no conflicts of interest to this work.

## Data Availability Statement

The data that support the findings of this study are openly available in ESRI's ArcGIS portal at http://www.arcgis.com using the following code: *Storm_drain = gis.content.get('07d6eb057e554c51832c4f0852ecf9c0').* The data are good as of June 12, 2023 and may have changed over time.

## Author Contribution Statement

**James O. Ekeh:** Conceptualization, Methodology, Software, Validation, Formal analysis, Investigation, Resources, Writing – review & editing, Visualization. **Manoj K. Jha:** Conceptualization, Methodology, Software, Validation, Formal analysis, Investigation, Resources, Data curation, Writing – original draft, Writing – review & editing, Visualization.

## References

[1] Centre for Research on the Epidemiology of Disasters, & United Nations Office for Disaster Risk Reduction. (2020). *The human cost of disasters: An overview of the last 20 years, 2000–2019*. Retrieved from: https://www.undrr.org/publication/human-cost-disasters-overview-last-20-years-2000-2019

[2] Bertrand-Krajewski, J.-L. (2021). Integrated urban stormwater management: Evolution and multidisciplinary perspective. *Journal of Hydro-environment Research*, *38*, 72–83. https://doi.org/10.1016/j.jher.2020.11.003

[3] Eldho, T. I., Zope, P. E., & Kulkarni, A. T. (2018). Urban flood management in coastal regions using numerical simulation and geographic information system. In P. Samui, D. Kim, & C. Ghosh (Eds.), *Integrating disaster science and management: Global case studies in mitigation and recovery* (pp. 205–219). Elsevier. https://doi.org/10.1016/B978-0-12-812056-9.00012-9

[4] Bremer, L. L., Keeler, B., Pascua, P., Walker, R., & Sterling, E. (2021). Nature-based solutions, sustainable development, and equity. In J. Cassin, J. H. Matthews, & E. L. Gunn (Eds.), *Nature-based solutions and water security: An action agenda for the 21st century* (pp. 81–105). Elsevier. https://doi.org/10.1016/B978-0-12-819871-1.00016-6

[5] Jones, D., & Jha, M. K. (2009). Green infrastructure: Assessing the benefits of bioretention over traditional stormwater management. In *Environmental Science and Sustainability: 2nd World Scientific and Engineering Academic and Society (WSEAS) International Conference on Natural Hazards*, 134–141.

[6] Webber, J. L., Fletcher, T., Farmani, R., Butler, D., & Melville-Shreeve, P. (2022). Moving to a future of smart stormwater management: A review and framework for terminology, research, and future perspectives. *Water Research*, *218*, 118409. https://doi.org/10.1016/j.watres.2022.118409

[7] Guo, J. C. Y. (2017). *Urban flood mitigation and stormwater management*. USA: CRC Press.

[8] Ekeh, J. (2020). *A GIS-based optimization model to minimize urban flood risk due to storm-drain system deficiencies*. PhD Thesis, Morgan State University.

[9] Atta-ur-Rahman, Parvin, G. A., Shaw, R., & Surjan, A. (2016). Cities, vulnerability, and climate change. In R. Shaw, Atta-ur-Rahman, A. Surjan, & G. A. Parvin (Eds.), *Urban disasters and resilience in Asia* (pp. 35–47). Butterworth-Heinemann. https://doi.org/10.1016/B978-0-12-802169-9.00003-3

[10] Boulmaiz, T., Guermoui, M., Saber, M., Boutaghane, H., Abida, H., & Eslamian, S. (2023). Uncertainty analysis using fuzzy models in hydroinformatics. In S. Eslamian & F. Eslamian (Eds.), *Handbook of hydroinformatics: Volume I: Classic soft-computing techniques* (pp. 423–434). Elsevier. https://doi.org/10.1016/B978-0-12-821285-1.00002-6

[11] Cook, S., van Roon, M., Ehrenfried, L., LaGro Jr, J., & Yu, Q. (2019). WSUD "best in class"—Case studies from Australia, New Zealand, United States, Europe, and Asia. In A. K. Sharma, T. Gardner, & D. Begbie (Eds.), *Approaches to water sensitive urban design* (pp. 561–585). Woodhead Publishing. https://doi.org/10.1016/B978-0-12-812843-5.00027-7

[12] Lopez-Gunn, E., Altamirano, M. A., Ebeltoft, M., Graveline, N., Marchal, R., Moncoulon, D., . . . , & Cassin, J. (2021). Mainstreaming nature-based solutions through insurance: The five "hats" of the insurance sector. In J. Cassin, J. H. Matthews, & E. Lopez Gunn (Eds.), *Nature-based solutions and water security: An action agenda for the 21st century* (pp. 401–422). Elsevier. https://doi.org/10.1016/B978-0-12-819871-1.00006-3

[13] Meng, C. L. (2018). A review of road surface conditions forecast. In *Elsevier reference collection in earth systems and environmental sciences.* Elsevier. https://doi.org/10.1016/B978-0-12-409548-9.11483-6

[14] Myers, B. R., & Pezzaniti, D. (2019). Flood and peak flow management using WSUD systems. In A. K. Sharma, T. Gardner, & D. Begbie (Eds.), *Approaches to water sensitive urban design: Potential, design, ecological health, urban greening, economics, policies, and community perceptions* (pp. 119–138). Woodhead Publishing. https://doi.org/10.1016/B978-0-12-812843-5.00006-X

[15] Sebastian, A., Juan, A., & Bedient, P. B. (2022). Urban flood modeling: Perspectives, challenges, and opportunities. In S. Brody, Y. Lee, & B. B. Kothuis (Eds.), *Coastal flood risk reduction* (pp. 47–60). Elsevier. https://doi.org/10.1016/B978-0-323-85251-7.00005-6

[16] Sinha, S. (2023). Climate change, urban flooding, and community perceptions of vulnerability and resilience: Lessons from Diamond Harbor region. In U. Chatterjee, R. Shaw, G. S. Bhunia, & S. Banerjee (Eds.), *Climate change, community response and resilience: Insight for socio-ecological sustainability: Volume 6 in developments in weather and climate science* (pp. 391–417). Elsevier. https://doi.org/10.1016/B978-0-443-18707-0.00021-7

[17] Upreti, M., Saikia, P., Shilky, Lal, P., & Kumar, A. (2024). Major challenges in the urbanizing world and role of earth observations for livable cities. In A. Kumar, P. K. Srivastava, P. Saikia, & R. K. Mall (Eds.), *Earth observation in urban monitoring: Techniques and challenges: A volume in earth observation* (pp. 23–52). Elsevier. https://doi.org/10.1016/B978-0-323-99164-3.00002-1

[18] Jha, M. K., & Schonfeld, P. (2000). Integrating genetic algorithms and geographic information system to optimize highway alignments. *Transportation Research Record: Journal of the Transportation Research Board*, *1719*(1), 233–240. https://doi.org/10.3141/1719-31

[19] Chang, L.-F., & Huang, S.-L. (2015). Assessing urban flooding vulnerability with an emergy approach. *Landscape and Urban Planning*, *143*, 11–24. https://doi.org/10.1016/j.landurbplan.2015.06.004

[20] Cherqui, F., Belmeziti, A., Granger, D., Sourdril, A., & le Gauffre, P. (2015). Assessing urban potential flooding risk and identifying effective risk-reduction measures. *Science of the Total Environment*, *514*, 418–425. https://doi.org/10.1016/j.scitotenv.2015.02.027

[21] Kim, Y., Eisenberg, D. A., Bondank, E. N., Chester, M. V., Mascaro, G., & Underwood, B. S. (2017). Fail-safe and safe-to-fail adaptation: Decision-making for urban flooding under climate change. *Climatic Change*, *145*, 397–412. https://doi.org/10.1007/s10584-017-2090-1

[22] Xie, J., Chen, H., Liao, Z., Gu, X., Zhu, D., & Zhang, J. (2017). An integrated assessment of urban flooding mitigation strategies for robust decision making. *Environmental Modelling & Software*, *95*, 143–155. https://doi.org/10.1016/j.envsoft.2017.06.027

[23] Zhou, X., Bai, Z., & Yang, Y. (2017). Linking trends in urban extreme rainfall to urban flooding in China. *International Journal of Climatology*, *37*(13), 4586–4593. https://doi.org/10.1002/joc.5107

[24] EPA National Stormwater Calculator. (n.d.). *Help prevent pollution by controlling stormwater runoff.* Retrieved from: https://swcweb.epa.gov/stormwatercalculator

[25] Flynn, C. D., & Davidson, C. I. (2016). Adapting the social-ecological system framework for urban stormwater management: The case of green infrastructure adoption. *Ecology & Society*, *21*(4), 19. https://doi.org/10.5751/ES-08756-210419

[26] Hatt, B. E., Fletcher, T. D., Walsh, C. J., & Taylor, S. L. (2004). The influence of urban density and drainage infrastructure on the concentrations and loads of pollutants in small streams. *Environmental Management*, *34*, 112–124. https://doi.org/10.1007/s00267-004-0221-8

[27] Tzoulas, K., Korpela, K., Venn, S., Yli-Pelkonen, V., Kaźmierczak, A., Niemela, J., & James, P. (2007). Promoting ecosystem and human health in urban areas using Green Infrastructure: A literature review. *Landscape and Urban Planning*, *81*(3), 167–178. https://doi.org/10.1016/j.landurbplan.2007.02.001

[28] Villarreal, E. L., Semadeni-Davies, A., & Bengtsson, L. (2004). Inner city stormwater control using a combination of best management practices. *Ecological Engineering*, *22*(4–5), 279–298. https://doi.org/10.1016/j.ecoleng.2004.06.007

[29] Duan, H.-F., Li, F., & Yan, H. (2016). Multi-objective optimal design of detention tanks in the urban stormwater drainage system: LID implementation and analysis. *Water Resources Management*, *30*, 4635–4648. https://doi.org/10.1007/s11269-016-1444-1

[30] Jun, C., Qin, X., Gan, T. Y., Tung, Y.-K., & de Michele, C. (2017). Bivariate frequency analysis of rainfall intensity and duration for urban stormwater infrastructure design. *Journal of Hydrology*, *553*, 374–383. https://doi.org/10.1016/j.jhydrol.2017.08.004

[31] Selbig, W. R., Fienen, M. N., Horwatich, J. A., & Bannerman, R. T. (2016). The effect of particle size distribution on the design of urban stormwater control measures. *Water*, *8*(1), 17. https://doi.org/10.3390/w8010017

[32] Monrabal-Martinez, C., Muthanna, T. M., & Meyn, T. (2016). Seasonal variation in pollutant concentrations and particle size distribution in urban stormwater-design implications for BMPs. In *9th International Conference on Planning and Technologies for Sustainable URBAN WATER Management,* 1–7.

[33] Chen, Y., Samuelson, H. W., & Tong, Z. (2016). Integrated design workflow and a new tool for urban rainwater management. *Journal of Environmental Management*, *180*, 45–51. https://doi.org/10.1016/j.jenvman.2016.04.059

[34] Mays, L. W. (1976). *Optimal layout and design of storm sewer systems.* PhD Thesis, University of Illinois at Urbana-Champaign.

[35] Taur, C.-K., Toth, G., Oswald, G. E., & Mays, L. W. (1987). Austin detention basin optimization model. *Journal of Hydraulic Engineering*, *113*(7), 860–878. https://doi.org/10.1061/(ASCE)0733-9429(1987)113:7(860)

[36] Afshar, M. H. (2008). Rebirthing particle swarm optimization algorithm: Application to storm water network design. *Canadian Journal of Civil Engineering*, *35*(10), 1120–1127. https://doi.org/10.1139/L08-056
[37] Durrans, S. R., Dietrich, K., Ahmad, M., & Haestad Methods, Inc. (2003). *Stormwater conveyance modeling and design*. USA: Haestad Press.
[38] Tamm, O., Saaremäe, E., Rahkema, K., Jaagus, J., & Tamm, T. (2023). The intensification of short-duration rainfall extremes due to climate change–Need for a frequent update of intensity–duration–frequency curves. *Climate Services*, *30*, 100349. https://doi.org/10.1016/j.cliser.2023.100349
[39] Watershed Engineering. (2004). *Course notes on watershed engineering from Cornell University*. Retrieved from: https://www.coursehero.com/sitemap/schools/11-Cornell-University/courses/342315-BEE4730/
[40] Boggs, P., & Tolle, J. (1995). Sequential quadratic programming. *Acta Numerica*, *4*, 1–51. https://doi.org/10.1017/S0962492900002518

**How to Cite:** Ekeh, J. O., & Jha, M. K. (2025). Minimizing Urban Flooding by Optimal Design of Drainage System Using Sequential Least Squares Quadratic Programming and Spatial Datasets. *Journal of Computational and Cognitive Engineering*, *4*(3), 366–376. https://doi.org/10.47852/bonviewJCCE42022507